Real-time observation of template-assisted colloidal aggregation and colloidal dispersion under an alternating electric field*

Li Chao-Rong(李超荣)†, Li Shu-Wen(李书文), Mei Jie(梅 洁),
Xu Qing(徐 庆), Zheng Ying-Ying(郑莹莹), and Dong Wen-Jun(董文钧)

Department of Physics, Center for Optoelectronics Materials and Devices, and Key Laboratory of Advanced Textile Materials & Manufacturing Technology of Ministry of Education, Zhejiang Sci-Tech University, Hangzhou 310018*, China*

(Received 21 January 2011; revised manuscript received 9 March 2011)

A fascinating colloid phenomenon was observed in a specially designed template-assisted cell under an alternating electrical field. Most colloidal particles experienced the processes of aggregation, dispersion and climbing up to the plateaus of the patterns pre-lithographed on the indium tin oxide glass as the frequency of the alternating electrical field increased. Two critical frequencies $f_{\rm crit1} \approx 15$ kHz and $f_{\rm crit2} \approx 40$ kHz, corresponding to the transitions of the colloid behaviour were observed. When $f < 15$ kHz, the particles were forced to aggregate along the grooves of the negative photoresist patterned template. When 15 kHz $< f <$ 40 kHz, the particle clusters became unstable and most particles started to disperse and were blocked by the fringes of the negative photoresist patterns. As the frequency increased to above 40 kHz, the majority of particles started to climb up to the plateaus of the patterns. Furthermore, the dynamics analysis for the behaviour of the colloids was given and we found out that positive or negative dielectrophoresis force, electrohydrodynamic force, particle–particle interactions and Brownian motion change with the frequency of the alternating electric field. Thus, changes of the related forces affect or control the behaviour of the colloids.

Keywords: template-assisted, aggregation, dispersion, dynamics analysis

PACS: 81.10.–h, 82.70.–y, 82.70.Dd, 82.70.Kj **DOI:** 10.1088/1674-1056/20/7/078102

1. Introduction

Due to the small spatial size and the short time scale of atomic or molecular systems, various physical phenomena like crystal nucleation and growth can hardly be observed directly. In contrast, a colloidal system can be observed directly because of its large size, concomitant slower time scale and the same order of molar elastic constants and many thermodynamic parameters as those in atomic solids.[1] Therefore, to some extent, the colloidal system is considered as a counterpart of the atomic system (or molecular system), which can be used to study cooperative phenomena that are not likely to be investigated directly in the atomic system, including nucleation, phase transition and defect dynamics.[2−5] Hence, colloidal dynamic systems are investigated experimentally in recent years. Among the various experimental techniques for the manipulation of colloidal particles by using external forces such as capillary action, magnetic and electric field force, the one using alternating electric field force to drive the particles to order and to transfer has acquired a prominent position.[6−10] In the last decade, Liu *et al.* investigated the dynamics of colloidal nucleation,[11] crystal growth,[12] two-dimensional melting[13] and colloidal phase transition[14] using the colloidal system under an alternating electric field (AEF). It was suggested that the colloidal particles moved with the electrohydrodynamic (EHD) flow to aggregate laterally and to form a 2D assembly, which can be controlled by tuning the frequency and the field strength of the alternating electric field. The EHD flow in the vicinity of a dielectric stripe deposited on a conducting plate had been investigated theoretically and experimentally, and a simple geometry for the EHD flow had been analyzed by Nadal and his coworkers.[15] All their studies were expected to be of help to design the surface-controlled flows and to understand the collective behaviours of the colloids near the de-

*Project supported by the National Natural Science Foundation of China (Grant Nos. 10874153 and 50773003), the Science Foundation of Zhejiang Sci-Tech University of China, and the Innovation Research Project for Graduate Student of Zhejiang Province of China (Grant No. YK 2009051).

†Corresponding author. E-mail: crli@zstu.edu.cn

© 2011 Chinese Physical Society and IOP Publishing Ltd

fective electrode under the perturbation of the stripe. Moreover, Nadel *et al.* revealed the existence of a critical frequency, below which most particles aggregated and above which the tightly organized formation turned into an explosion.[16] They suggested that the attractive EHD force dominated and drove particles to aggregate below the critical frequency, and the repulsive dipole force dominated and led the particles to explode from the colloidal ordering structure above a critical frequency. Kumacheva *et al.* probed colloids located on patterned substrates by using microscopic imaging, studied the long-range order in the crystals and quantified the influence of surface patterning on the crystal quality.[17] Yeh *et al.* suggested that the long-ranged attraction between colloidal particles, which caused the aggregation, was generated by the electric-field flow.[18] The flow arised as a result of spatial perturbations in the lateral current distribution, which were induced by the colloidal particles themselves and the patterns on the electrode. The external manipulation of the movement of the colloidal particles evoked the researchers' interesting on separating mixed particles[19] and designing the novel flow patterns[20] by tuning the frequency of an external non-uniform electric field. In order to enhance the inhomogeneity of the electric field, the common method was fabricating arrays on the electrode so as to generate the high field and the dielectrophresis (DEP), which could lead particles to move in a special way. Green[21] surveyed the dynamics of sub-micrometer particles using planar microelectrode arrays manufactured by direct-write electron-beam lithography with alternating current signal. They found that the particles would move toward (positive DEP) or away from (negative DEP) the high field regions depending on the frequency.[22] Along these lines of investigation, we designed more complex dielectric patterns on the electrode surface of a cell, which consisted of an indium tin oxide (ITO) glass plate, a surface patterned ITO glass and a hollowed silicon sheet. We surveyed the behaviour of charged particles in suspension, which were sealed in the cell. With the surface negative photoresist patterns, we tried to discover the influence of the external electric field frequency on the particle motion and to explain the colloidal movement resulting from the interactions between particles in the colloidal system. The results could be useful for understanding the interactions between colloids in similar situations and could supply experimental and theoretical data for the theory of colloidal kinetics.

2. Experimental method

Figure 1 shows the experimental setup. A monodispersed silica particle (diameter 1.50 μm, polydispersity $< 5\%$, 1.0 wt%, from Merck Chimie SAS) suspension was diluted with ultra-pure water (resistivity 18.25 $\mathrm{M}\,\Omega\cdot\mathrm{cm}^{-1}$, Millipore-Q) into 0.025 wt% solution and then pretreated with mixed ion exchange resin for almost 12 h. The diluted suspension, in which the surface potential ζ of the colloidal particles was adjusted to -6.5 mV (measured by a Delsa Nano C Sphere Analyzer, Nano Beckman Coulter Inc.) by ion exchange, was sealed into an interim cell, which consists of one ITO glass plate (thickness 1.2 mm, resistivity 5 $\Omega/\square$, from Mike Chemical Instruments Co. Ltd.) and a surface patterned ITO glass. A piece of silicon sheet (thickness 0.5 mm) with a hole of 5 mm in diameter was used as a spacer. Two copper wire electrodes (0.2 mm in diameter, 10 cm in length) were stuck on the conducting surface of ITO-coated glass planes using conductive adhesive. In our study, an alternating electric field was generated by a waveform signal generator (Nanjing Shengpu Technology Co., Ltd.).

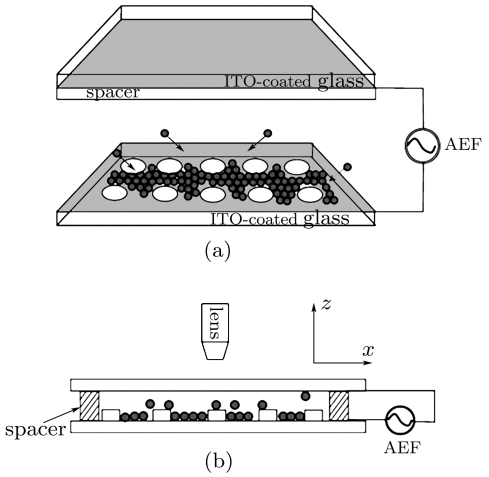


Fig. 1. Illustrations of experimental setup. (a) Cell structure. The colloidal suspension was sealed between two ITO-coated glasses separated by a piece of hollow silicon sheet spacer (Thickness: 0.5 mm; hole diameter: 5 mm) (b) Schematic diagram of experimental setup.

The applied frequency was varied from 1 kHz to 100 kHz and the voltage was fixed at 10 V. The real-time colloid motion was observed using a microscope (Olympus BX51) equipped with a 60× long working distance objective lens (0.7 mm numerical aperture, and 1.3 mm working distance) and a CCD camera (Micropublisher 5.0 RTV, a maximum resolution of 2560×1920, a pixel pitch of 3.4 μm × 3.4 μm, from QImaging). A frame imaging software (Image-pro

plus) was used to capture the process of particle ordering and transferring.

3. Results and discussion

3.1. Dynamics of colloidal ordering and the transferring process

A pure SiO_2 aqueous suspension was added into the sealed interim cell with a pre-patterned bottom ITO glass, as shown in Fig. 1. The patterns are shown in Fig. 2(a). When the colloidal suspension was sealed into the glass cell without the alternating electric field, the majority of particles were dispersed and involved in an intensive movement via Brownian motion (Fig. 2(b)). Once switching on the AEF (voltage 10 V, frequency 1 kHz), the colloidal particles dispersed in z direction rushed onto the surface of the bottom plane and rapidly aggregated in a very short time. A sequence of the aggregation of the colloids was captured and is shown in Figs. 2(b)–2(f). It was suggested that there was a strong attractive force induced by the AEF. Switching off the AEF, the aggregated structure started melting and the particles reversibly re-dispersed into the bulk. Several seconds after the beginning of our experiments, lots of particles remained in the grooves and a single particle was adsorbed to an optimal part of the front edge of the aggregated structure.[11]

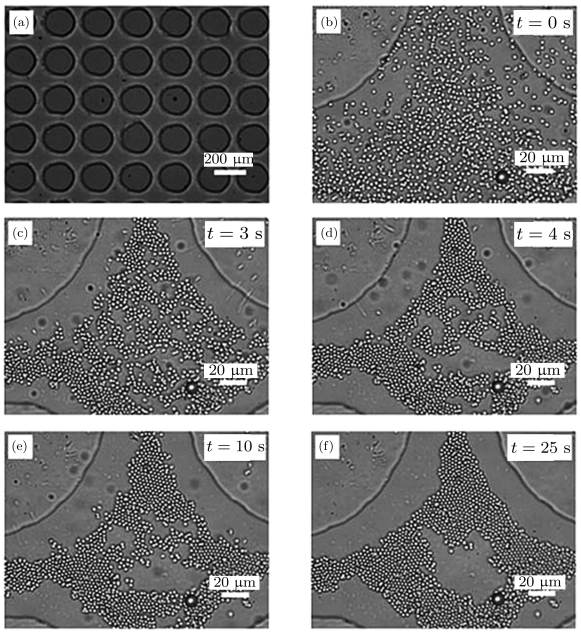


Fig. 2. An example of the aggregation of colloidal particles. (a) Microscopic image of patterns on an ITO-coated substrate. The height and the diameter of columns that form protuberant patterns are about 2 μm and 200 μm, respectively. (b) Without electrical field, particles move via Brownian motion. (c)–(f) Process of aggregation of colloidal particles in a groove under a given field ($f = 1$ kHz, $V = 10$ V).

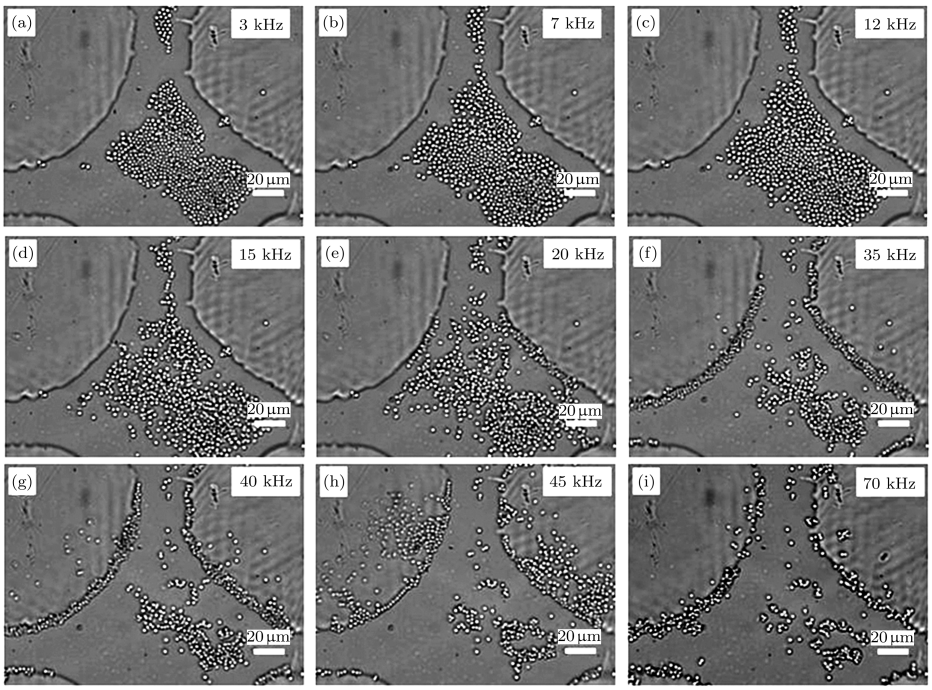


Fig. 3. Images of colloidal particles at different frequencies. Images captured at (a) $f = 3$ kHz, (b) $f = 3$ 7 kHz, (c) $f = 3$ 12 kHz, (d) $f = 3$ 15 kHz, (e) $f = 3$ 20 kHz, (f) $f = 3$ 35 kHz, (g) $f = 3$ 40 kHz, (h) $f = 3$ 45 kHz, (i) $f = 3$ 70 kHz.

Rather than stick to the negative photoresist patterns, particles preferred to assemble a little far away from the fringes of the negative photoresist patterns (Fig. 2(b)). It was suggested that the existence of microflows along the fringes of patterns swept the particles and forced them to aggregate in the intersectional regions, where the particles could stay at a relatively steady state.

By only increasing the frequency from 1 kHz to 15 kHz at a given voltage of 10 V, the silica particles were always incorporated in the growth of ordered monolayer (Fig. 2 and Figs. 3(a)–3(c)). For example, in Figs. 2(c) and 3(a), the particles congregate in the grooves of the protuberant pattern. Once the value of the frequency reached 15 kHz, the ordering clusters became dispersive. Obviously, the critical frequency around 15 kHz was a turning point, at which most particles had aggregated and formed packed planar clusters along the grooves of the negative photoresist patterns. At the critical frequency, particles began to disperse from clusters but were blocked by the protuberant photoresist patterns. Most particles were kept at the fringes of the negative photoresist patterns (Figs. 3(a)–3(c)).

As frequency increased to another critical value ($f_{\rm crit2}$ is around 40 kHz), a vast majority of particles started to climb up to the plateaus of the patterns rather than assemble in the grooves (Figs. 3(d) and 3(e)). This behaviour of the particles continued to the frequency of 70 kHz, at which a few particles that had climbed up to the plateaus drifted away from the vision of the optical microscope (Fig. 3(f)). The phenomenon lasted until the frequency reaches the maximum value of 100 kHz. The related mechanisms will be discussed in detail in the next section.

3.2. Mechanism of colloidal ordering and the transferring process

When the colloidal suspension was sealed into two conducting ITO-coated glass plates under an alternating electric field, the colloids experienced forces derived from three aspects: particle–particle interactions, particle–solution interactions and the external field.[23] In particular, the behaviours of the colloidal particles were mainly controlled by dipole-dipole interaction, electrostatic force, gravity, buoyancy, forces induced by the external electric field, viscous drag force from the solution and Brownian motion. When switching on the electric field, an ion polarization occurred on the surface of the charged particles, thus resulting in a dipole vector $\bar{\boldsymbol{\mu}}(\omega)$ (Fig. 4), which was perpendicular to the bottom of the ITO glass. The interaction between the non-uniform ac electric field and the dipole moment drove the particles to move. This movement is called dielectrophoresis (DEP).[24] The resulting DEP force can be given by[25]

$$\bar{\boldsymbol{F}}_{\rm DEP} = {\rm Re}[(\bar{\boldsymbol{\mu}}(\omega)\cdot\boldsymbol{\nabla})\bar{\boldsymbol{E}}], \tag{1}$$

where $\bar{\boldsymbol{E}}$ is the electric field, $\bar{\boldsymbol{\mu}}(\omega)$ is the induced dipole moment of the particles, Re indicates the real part. For a spherical particle, the induced dipole vector is $\bar{\boldsymbol{\mu}}(\omega) = V\alpha(\omega)\bar{\boldsymbol{E}}$, where ω is the electric field angular frequency $\omega = 2\pi\nu$, $\alpha(\omega)$ is the effective polarizability of the particle $\alpha(\omega) = 3\varepsilon_{\rm m}K(\omega)$, $\varepsilon_{\rm m}$ is the permittivity of the medium, V is volume of the particle $V = 4\pi a^3/3$, a is the particle radius. Thus the dipole moment is given by

$$\bar{\boldsymbol{\mu}}(\omega) = 4\pi a^3\varepsilon_{\rm m}K(\omega)\bar{\boldsymbol{E}}, \tag{2}$$

where $K(\omega)$ is the Clausius–Mossotti factor $K(\omega) = (\varepsilon_{\rm p}^* - \varepsilon_{\rm m}^*)/(\varepsilon_{\rm p}^* + 2\varepsilon_{\rm m}^*)$, $\varepsilon_{\rm p}^*$ and $\varepsilon_{\rm m}^*$ are permittivities of the particle and the medium, respectively. The ε^* is given by $\varepsilon^* = \varepsilon - {\rm j}\sigma/\omega$, where ${\rm j} = \sqrt{-1}$, σ is the conductivity of the dielectric.

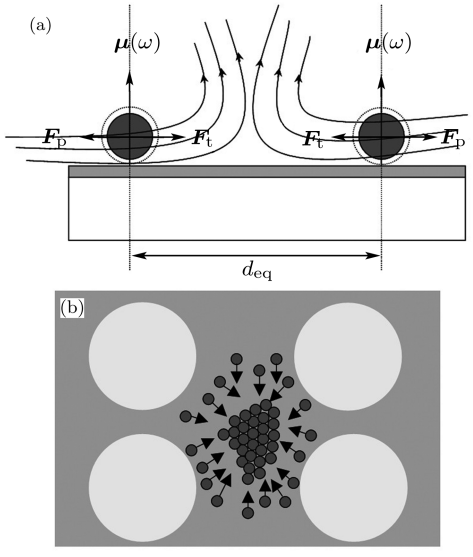


Fig. 4. (a) Schematic diagram of the interaction between two particles. (b) Top view of the particle motion under the applied electric field (frequency: 1 kHz $< f <$ 15 kHz, voltage is 10 V).

For the particles, the average force is given by

$$\langle \boldsymbol{F}_{\rm DEP}\rangle = \frac{1}{2}\,{\rm Re}\,[(\bar{\boldsymbol{\mu}}(\omega)\cdot\boldsymbol{\nabla})\bar{\boldsymbol{E}}^*]. \tag{3}$$

Considering the irrotational field and the Gauss theorem, the $\boldsymbol{F}_{\rm DEP}$ can be rewritten by

$$\langle \boldsymbol{F}_{\rm DEP} \rangle = \frac{1}{4} V \,{\rm Re}\,[\alpha(\omega) \boldsymbol{\nabla} (\bar{\boldsymbol{E}} \cdot \bar{\boldsymbol{E}}^*)] - \frac{1}{2} V \,{\rm Im}\,[\alpha(\omega) \boldsymbol{\nabla} \times (\bar{\boldsymbol{E}} \times \bar{\boldsymbol{E}}^*)]. \quad (4)$$

The first term on the right-hand side of Eq. (4) is the traditional $\boldsymbol{F}_{\rm DEP}$ and can be considered as the total $\boldsymbol{F}_{\rm DEP}$ when there is only spatial variation of the field magnitude but no variation of the potential phase. The second term is regarded as the travelling wave $\boldsymbol{F}_{\rm DEP}$ and exists when there is spatial variation of both the field magnitude and the potential phase.

In our experiments, the negative photoresist patterns resulted in plateaus and grooves on the bottom electrode. As there is no variation of the potential phase, the $\boldsymbol{F}_{\rm DEP}$ can be expressed as

$$\langle \boldsymbol{F}_{\rm DEP} \rangle = \pi \varepsilon_{\rm m} a^3 \,{\rm Re}\,[K(\omega)] \boldsymbol{\nabla} |E|^2. \quad (5)$$

Apart from the dielectrophoresis force, the particles were also affected by the electrohydrodynamic force arising from the fluid movement due to electrohydrodynamic effects. For a spherical particle, the electrohydrodynamic force is approximated by Stoke's force,[15] which is $\boldsymbol{F}_{\rm EHD} \sim 6\pi\eta a \boldsymbol{\upsilon}(f, r)$, where η is water viscosity, a is the average particle radius, $\boldsymbol{\upsilon}(f, r)$ is a frequency-dependent EHD velocity at a given distance r from one of the particles.

From Eq. (5), it is easy to find that the traditional $\boldsymbol{F}_{\rm EDP}$ depends on the parameter ${\rm Re}[K(\omega)]$, which depends on the applied frequency. The value of ${\rm Re}[K(\omega)]$ varies from +1 to –1/2 and exists a turning point, at which the value change from positive to negative.[26] Corresponding to the change of ${\rm Re}[K(\omega)]$, the direction of the dielectrophoresis force will reverse with the tuning of the frequency.

Compared with other forces, $\boldsymbol{F}_{\rm DEP}$, $\boldsymbol{F}_{\rm EHD}$, particle–particle forces ($\boldsymbol{F}_{\rm p}$) and Brownian motion dominate the particle movement.[22] Moreover, all these main forces are frequency-dependent, which means that the behaviour of the particles would change with the frequency of the applied electric field.[27]

In order to find the effect of the main interactions on our colloidal system, we used the double-particles model to describe the interactions between particles (Fig. 4(a)).

When the colloidal suspension was sealed between two conducting ITO-coated glass plates, there were two interactions competing with each other. If one of the two had advantage over the other, the winner would lead colloidal particles to move. At the beginning of adding colloidal suspension to the experimental cell without the AEF, there was an initial distance between the particles, which was related to the concentration of the colloid suspension. Upon switching on the AEF, the dipole vector $\boldsymbol{\mu}(\omega)$ (Fig. 4(a)), which was perpendicular to the bottom electrode, was generated as a result of the ion polarization occurring at the surface of the charged particles. In addition, due to the charge layer around the surface of the particles, there was a repulsive interaction $\boldsymbol{F}_{\rm p}$ between the particles (see Fig. 4(a)). Evidently, the aggregation was not the result of the repulsive force, the total strength of the other forces was strong enough to overcome the repulsive particle–particle interactions $\boldsymbol{F}_{\rm p}$ and the Brownian motion.[28] The total attractive interaction $\boldsymbol{F}_{\rm t}$ depended on the above two interactions $\boldsymbol{F}_{\rm DEP}$ and $\boldsymbol{F}_{\rm EHD}$ ($\boldsymbol{F}_{\rm t} \sim \boldsymbol{F}_{\rm DEP} + \boldsymbol{F}_{\rm EHD}$), with $\langle \boldsymbol{F}_{\rm DEP} \rangle = \pi \varepsilon_{\rm m} a^3 {\rm Re}[K(\omega)] \boldsymbol{\nabla} |E|^2$ and $\boldsymbol{F}_{\rm EHD} \sim 6\pi\eta a \boldsymbol{\upsilon}(f, r)$. In our colloidal system, the viscosity and the radius were constant values. The $\boldsymbol{\upsilon}(f, r)$ only depended on the frequency when the distance r between the two particles was a given value. Remarkably, the initial distance between the particles was so large that the electrostatic repulsive interaction was negligible. When setting the initial f at 1 kHz, since the instantaneous $\boldsymbol{F}_{\rm t}$ was stronger than $\boldsymbol{F}_{\rm p}$, the majority of particles would be forced to aggregate. The aggregation was caused by the long-range attraction induced by the cooperation between the attractive forces and the repulsive forces, which included $\boldsymbol{F}_{\rm p}$ and Brownian motion. As shown in Figs. 2(b) and 2(c), the particles aggregated in a very short time. When the majority of particles aggregated together and reached a state of equilibrium, the distance between particles was a given value $d_{\rm eq}$ and $\boldsymbol{F}_{\rm t}$ was balanced by the cooperated interaction of $\boldsymbol{F}_{\rm p}$ and Brownian motion. From the study of Ristenpart *et al.*,[29] we know that the value of $\boldsymbol{F}_{\rm EHD}$ monotonically decreases with the increase of the frequency and decays as r^{-4} at low frequency regime (1 kHz$< f <$15 kHz).[30] By increasing frequency from 1 kHz to the $f_{\rm crit1}$ (15 kHz), $\boldsymbol{F}_{\rm EHD}$ decreased, the variation of the particle polarization caused ${\rm Re}[K(\omega)]$ to change from + to –, thus the dielectrophoresis force $\boldsymbol{F}_{\rm DEP}$ changed from positive to negative at the first critical frequency, and then the cooperative interaction of $\boldsymbol{F}_{\rm DEP}$ and $\boldsymbol{F}_{\rm p}$ had a tendency to become stronger than $\boldsymbol{F}_{\rm EHD}$, which led the particle clusters into a noncontact steady structure (Fig. 3(a)). By continuously increasing the frequency from 15 kHz

to the high frequency regime, $\boldsymbol{F}_{\rm DEP}$, which had become repulsive force, was stronger than the attractive interaction $\boldsymbol{F}_{\rm EHD}$ and then the dominating repulsive forces $\boldsymbol{F}_{\rm DEP}$, $\boldsymbol{F}_{\rm p}$ and Brownian motion led to the further dispersion of the particles (Fig. 3(b)).

As the frequency increased from 15 kHz to 40 kHz, the distances between the particles became so large that $\boldsymbol{F}_{\rm p}$ was negligible. The particles were blocked by the protuberant photoresist patterns when the cooperative force of $\boldsymbol{F}_{\rm EHD}$ and $\boldsymbol{F}_{\rm DEP}$ was not strong enough. But with the increasing of the frequency and the distance between the particles, $\boldsymbol{F}_{\rm EHD}$ decreased and thus the cooperative force of $\boldsymbol{F}_{\rm DEP}$ and $\boldsymbol{F}_{\rm EHD}$ could generate a strong enough moment for the particles so that most particles climbed up to the plateaus from the low grooves. More specifically, by the combination of $\boldsymbol{F}_{\rm DEP}$ and $\boldsymbol{F}_{\rm EHD}$, the particles were collected at the plateaus of the patterns (Fig. 5).

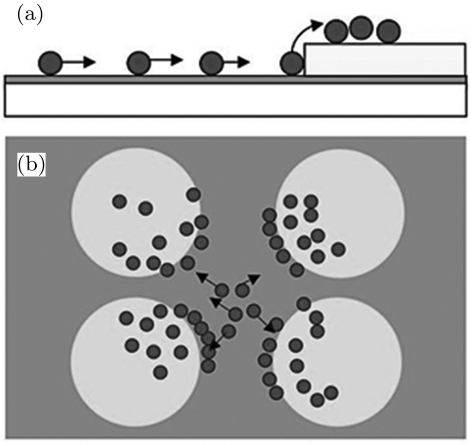


Fig. 5. Schematic of the particle motion from the fringes of the patterns to the plateaus of the patterns on the bottom electrode. (a) Lateral view of the particle movement. (b) Top view of the particle movement.

Although the processes of colloidal aggregation, colloidal dispersion and climbing up to the plateaus of the negative patterns were observed, and we do have a good explanation for the phenomena, the mechanism is still not completely clear up to now and needs further investigation.

4. Conclusion

A novel template-assisted colloidal self-assembly approach was designed to study template-assisted colloidal aggregation and colloidal dispersion under an alternating electric field. The process of colloidal particle ordering and transferring was recorded. The influences of both the alternating electric field and the electrode-surface patterns on the colloidal behaviours have been studied. The long-range interaction induced by the cooperation of $\boldsymbol{F}_{\rm EHD}$, particle–particle interactions $\boldsymbol{F}_{\rm p}$ and positive $\boldsymbol{F}_{\rm DEP}$ led the particles to aggregate and to form packed planar clusters along the grooves of the negative photoresist patterns at low frequency (1 kHz $< f <$ 15 kHz). By tuning frequency from 15 kHz to the high frequency regime (15 kHz $< f <$ 70 kHz), most of the particles dispersed from the ordered clusters and climbed up to the plateaus of the patterns from the low grooves by the combination of $\boldsymbol{F}_{\rm DEP}$ and $\boldsymbol{F}_{\rm EHD}$, $\boldsymbol{F}_{\rm p}$ and Brownian motion. The method used in this study will be useful to design more complex surface controlled fluid flow and the result could be a supplement for the theory of colloidal kinetics under an alternating electric field.

References

[1] Arora A K and Tata B V R 1996 *Ordering and Phase Transitions in Charged Colloids* (New York: VCH publisher Inc.) p. 1
[2] Zhang K Q and Liu X Y 2004 *Nature* **429** 739
[3] Zhang K Q and Liu X Y 2006 *Phys. Rev. Lett.* **96** 105701
[4] Xie R G and Liu X Y 2009 *J. Am. Chem. Soc.* **131** 4976
[5] Feng T H, Dai Q F, Wu L J, Guo Q, Hu W and Lan S 2008 *Chin. Phys.* B **17** 4533
[6] Denkov N D, Velev O D, Kralchevsky P A, Ivanov I B, Yoshimura H and Nagayama K 1992 *Langmuir* **8** 3183
[7] Erb R M, Son1 H S, Samanta B, Rotello V M and Yellen B B 2009 *Nature* **457** 999
[8] Williams S J, Kumar A and Wereley S T 2009 *Phys. Fluids* **21** 091104
[9] Yan H T, Wang M, Ge Y X and Yu P 2009 *Chin. Phys.* B **18** 2389
[10] Zhang L F and Huang J P 2010 *Chin. Phys.* B **19** 024213
[11] Zhang T H and Liu X Y 2009 *Angew. Chem. Int. Ed.* **48** 1308
[12] Zhang T H and Liu X Y 2007 *J. Phys. Chem.* C **111** 1342
[13] Zhang T H and Liu X Y 2006 *Appl. Phys. Lett.* **89** 261914
[14] Liu Y, Narayanan J and Liu X Y 2006 *J. Chem. Phys.* **124** 124906
[15] Nadal F, Argoul F, Kestener P, Pouligny B, Ybert C and Ajdari A 2002 *Eur. Phys. J.* E **9** 387
[16] Nadal F, Argoul F, Hanusse P, Pouligny B and Ajdari A 2002 *Phys. Rev.* E **65** 061409
[17] Allard M, Sargent E H, Lewis P C and Kumacheva E 2004 *Adv. Mater.* **16** 15
[18] Yeh S R, Seul M and Shraiman B I 1997 *Nature* **386** 57
[19] Kaler K, Xie J P, Jones T B and Paul R 1992 *Biophys. J.* **63** 58
[20] Ramos A, Morgan H, Green N G and Castellanos A 1999 *J. Colloid Interface Sci.* **217** 420
[21] Green N G and Morgan H 1998 *J. Phys.* D: *Appl. Phys.* **31** L25
[22] Green N G, Ramos A and Morgan H 2000 *J. Phys.* D: *Appl. Phys.* **33** 632

[23] Li J F, Yu W H, Chen C S and Wei W C 2003 *Technical Proceedings of the 2003 Nanotechnology Conference and Trade Show*, San Francisco, Febuary 2, 2003 p. 566

[24] Pohl H A 1951 *J. Appl. Phys.* **22** 869

[25] Jones T B 1995 *Electromechanics of Particles* (New York: Cambridge University Press) pp. 5–82

[26] Green N G and Morgan H 1997 *J. Phys.* D: *Appl. Phys.* **30** L41

[27] Russel W B, Saville D A and Schowalter W R 1989 *Colloidal Dispersions* (New York: Cambridge University Press) pp. 1–454

[28] Trau M, Saville D A and Aksay I A 1997 *Langmuir* **13** 6375

[29] Ristenpart W D, Aksay I A and Saville D A 2004 *Phys. Rev.* E **69** 021405

[30] Ristenpart W D, Aksay I A and Saville D A 2007 *J. Fluid Mech.* **575** 83